International Journal of Mechanical, Industrial and Aerospace Sciences
ISSN: 2517-9950
Vol:10, No:5, 2016

Study the Effect of Roughness on the Higher Order Moment to Extract Information about the Turbulent Flow Structure in an Open Channel Flow

Md Abdullah Al Faruque, Ram Balachandar

***Abstract*—**The present study was carried out to understand the extent of effect of roughness and Reynolds number in open channel flow (OCF). To this extent, four different types of bed surface conditions consisting smooth, distributed roughness, continuous roughness, natural sand bed and two different Reynolds number for each bed surfaces were adopted in this study. Particular attention was given on mean velocity, turbulence intensity, Reynolds shear stress, correlation, higher order moments and quadrant analysis. Further, the extent of influence of roughness and Reynolds number in the depth-wise direction also studied. Increasing Reynolds shear stress near rough beds are noticed due to arrays of discrete roughness elements and flow over these elements generating a series of wakes which contributes to the generation of significantly higher Reynolds shear stress.

***Keywords*—**Bed roughness, ejection, sweep, open channel flow, Reynolds Shear Stress, turbulent boundary layer, velocity triple product.

I. Introduction

THE structure and dynamics of open channel flow which comprises a shear/boundary layer like flow is of vital importance to the modeling of sediment transport and resuspension, bed formation, entrainment and the exchange of energy and momentum. Processes of special interest within the flow include the horizontal and vertical transfer of energy and momentum by turbulence. For example, in the case of some benthic organisms, nutrition/oxygen utilization rates are known to vary with flow conditions. Increasing current speed enhances vertical diffusive transport of phytoplankton due to increased turbulent mixing. Although the mechanisms concerning the above mentioned phenomena have been studied in the past, they are not completely understood. Reference [1] indicates that even average particle volume fractions as low as 10^{-4} lead to a significant modulation of turbulence. The shape, size and arrangement of bed particles also contribute to the modulation of turbulence. In contrast to the vast research on turbulent boundary layer and pipe flow, research in open channel turbulence has only been conducted since 1970s. Since then, extensive experimental and theoretical turbulent flows over smooth surfaces have been completed [2]-[8]. Flow over a rough surface has significance in many engineering applications. However, as rightly pointed by [9], flow over rough surface continues to be the Achilles heel of turbulence research. The suggested use of turbulent boundary layer data for modeling open channel flow is debatable due to basic differences between the two; influenced by the channel aspect ratio and the presence of the free surface [10]. Formation and enhancement of secondary currents occur due to the presence of free surface and the side walls of the open channel. Free surface also dampens the vertical velocity fluctuations.

Reference [11] studied the flow progression from a developing state to a fully developed condition and noted that along the axis of a fully developed section, the boundary layer extends to the water surface if the aspect ratio $b/d \geq 3$. Near the free surface, they did not observe any dip in the velocity profile at the channel centerline even for channel with aspect ratio as low as $b/d = 3$. Reference [12] showed that roughness effects on the velocity field were similar to those observed in a zero-pressure gradient turbulent boundary layer, even though the boundary layer in an open channel flow is influenced by the free surface. Reference [6] related the aspect ratio (width/depth ratio of flow, b/d) to the formation of secondary currents and noted that the maximum velocity on the centerline occurred below the free surface for $b/d < 5$ (velocity-dip phenomenon). Reference [13] indicated that the streamwise mean velocity profiles follow the well-known logarithmic law for the smooth surface, and with an appropriate shift, for the rough surface. Reference [14] observed that wall roughness led to higher turbulence levels in the outer region of the boundary layer. Reference [12] noted that roughness enhances the levels of the turbulence intensities over most of the flow.

Reference [15] noted that the coherent wall structures are the dominant factor affecting particle motion near a solid boundary, as well as influencing deposition and entrainment. They also noted that the vortices generate high-speed regions relative to the fluid in the viscous layer, sweep along the wall, pushing particles out of the way. Reference [16] reported that for locations above the roughness sublayer, the distributions of the second-order turbulent stresses are similar to the smooth-wall distributions. Reference [12] noted that roughness enhances the levels of the Reynolds shear stress over most of the flow. Reference [17] noted that surface roughness significantly enhances the levels of the Reynolds stresses in a

Md Abdullah Al Faruque (Associate Professor) is with the Civil Engineering Technology, Rochester Institute of Technology, 78 Lomb Memorial Drive, Rochester, NY 14623 USA (corresponding author, phone: 1-585-475-6664; fax: 1-585-475-7964; e-mail: aafite@rit.edu).

Ram Balachandar (Associate Vice Provost and Executive Director) is with the Centre for Executive and Professional Education, Professor, Faculty of Engineering, University of Windsor, 401 Sunset Ave., Windsor, ON Canada N9B 3P4 (e-mail: rambala@uwindsor.ca).

way that depends on the specific geometry of the roughness elements. They also noted that, surface roughness enhances the level of the Reynolds stresses over most of the flow and suggest a stronger interaction between the inner and outer regions of the flow than would be implied by the wall similarity hypothesis.

Reference [6] predicted that the Reynolds shear stress ($-\overline{uv}$) might become negative near the free surface if the flow become three-dimensional (when b/d ≤ 5). He emphasized the importance of the correlation coefficient of the Reynolds stress because it involved only turbulence quantities, without the need for estimating friction velocity. Correlation coefficient of the Reynolds stress indicates the degree of similarity of turbulence and could be defined as $R = -\overline{uv}/(u'v')$. Here, u' and v' is the turbulence intensity in streamwise direction and normal to the bed, respectively. Reference [6] noted that the value of R increases monotonously with y/d in the wall region, decreases in the free-surface region and remains nearly constant, at about 0.4~0.5, in the intermediate region ($0.1 \leq y/d \leq 0.6$). He also noted that the distribution of R is universal, i.e., it is independent of the properties of mean flow and the wall roughness. Reference [18] noted that the Reynolds stress attains a maximum and decreases towards the bed in the wall region. They explained that in the case of smooth walls, this behavior was due to the viscous effects, while for rough walls it was due to the existence of a roughness sublayer where additional mechanisms for momentum extraction emerge. They noticed contradicting behavior of Reynolds stress with variation of Reynolds number and associated this to secondary currents due to a relatively lower value of aspect ratio.

Reference [19] reported that the relative contributions of sweep and ejection events within the sublayer showed that sweep events provide the dominant contribution to the Reynolds shear stress within this region. Reference [12] noted that triple correlations and turbulence diffusion were strongly modified by the surface roughness. Reference [17] noted that surface roughness significantly enhances the levels of the turbulence kinetic energy, and turbulence diffusion in a way that depends on the specific geometry of the roughness elements. Reference [7] showed that the triple products are sensitive to the wall condition and the effects are prevalent throughout the depth of flow. They noted that ejection events are dominant throughout the depth and also vary significantly with wall roughness. From the velocity quadrant decomposition, they also noted that the magnitudes of the extreme events are higher for the rough wall in comparison to smooth wall throughout the depth. This indicates that effect of bed roughness is not limited to the region close to the bed. Reference [10] showed from the quadrant analysis that the turbulent structures in the outer region of the open channel is similar to the structures noted in turbulent boundary layers, but only for the case where all turbulent events were included. They observed significant differences between open channel flow and turbulent boundary when only the extreme events are considered.

II. Experimental Setup

A 9-m long rectangular open channel flume (cross-section 1100 mm x 920 mm) was used to carry out the experiments. Fig. 1 shows the schematic drawing of the open channel flume and experimental setup used in this study. Transparent tempered glass was used to construct the sidewalls and bottom of the flume to facilitate velocity measurements using a laser Doppler anemometer. The same flume was used in various previous studies and it is a permanent facility. The slope of the channel bottom is adjustable and the quality of flow has been confirmed in previous studies. The channel bottom was set to be horizontal for the present experiments. A summary and details of test conditions can be found in [20] and avoided here for brevity. A rectangular header tank of the cross-section of 1.2 m square and 3.0 m deep was placed in the upstream of the flume. The flow depth (d) was kept constant to 100 mm in the measurement region, resulting in a width-to-depth ratio (b/d) of approximately 11. The flow is considered to be nominally two-dimensional [6] because the aspect ratio of 11 is considered to be large enough to minimize the effect of secondary currents. To condition the flow, flow straighteners were used at the beginning and the end of flume. The flow conditions were maintained in such a manner that there was no initiation of sand movement. However, a sand trap was provided at the downstream of the bed to prevent any accidental transport of sand particles into the pump/piping assembly.

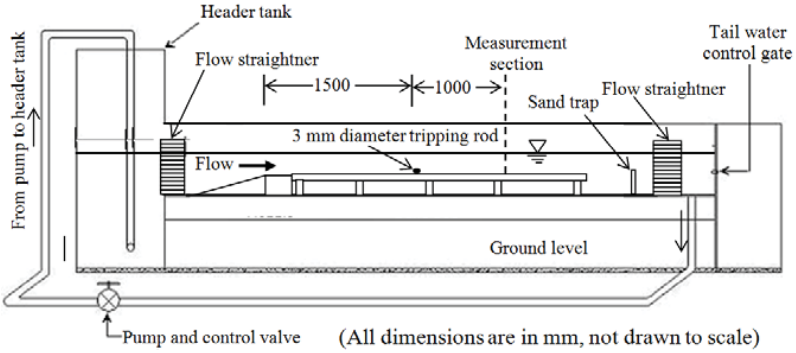

Fig. 1 Schematic of the open channel flume and experimental setup

One smooth bed and three different rough types of bed surface conditions were used in this study. A hydraulically smooth surface generated using a 3.7 m long polished aluminum plate spanning the entire width of flume (Fig. 2 (a)) and use it as a base case. Sand particles (d_{50} = 2.46 mm, $\sigma_g = \sqrt{d_{84}/d_{16}}$ = 1.24) were used to create the three different types of rough surfaces. To generate the first rough surface (designated as 'distributed roughness'), 18-mm wide sand strips were glued to the smooth aluminum plate alternating with 18-mm wide smooth strips as shown in Fig. 2 (b). The second roughness condition consisted of the same sand grains glued over the entire smooth surface as shown in Fig. 2 (c) (continuous roughness). In both cases the sand was affixed to the aluminum plate in a single grain layer. Third rough surface was generated using 200-mm thick and 3.7 m long uniform sand bed as shown in Fig. 3.

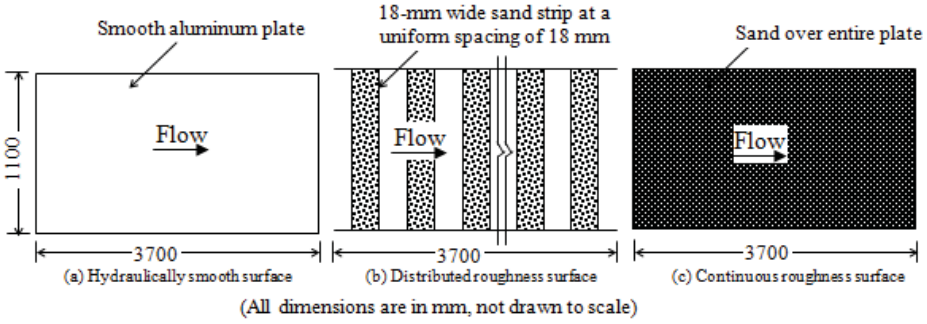

Fig. 2 Plan view of different fixed bed condition

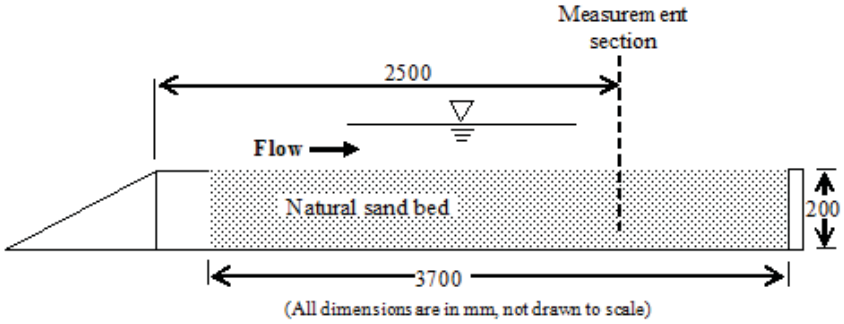

Fig. 3 Section of natural sand bed

The tripping of the boundary layer was required to achieve a fully developed turbulent flow in the test region for tests over the smooth bed. A 3-mm diameter rod was used as a trip upstream of the measurement region to ensure the presence of a turbulent boundary layer. The boundary layer shape factor for the smooth bed is found to be ≈ 1.3, which can be defined as the ratio of displacement to momentum thickness, which is an indication of fully developed turbulent flow [21] for tests over the smooth bed. The measurements for the distributed roughness were conducted on top of 60th sand strip. To minimize secondary flow effects, all the measurements were conducted along the centreline of the channel. Preliminary tests were conducted to ensure a fully developed flow condition.

Two different Reynolds numbers (based on depth of flow) were used for each test condition. Reynolds numbers were chosen in order to keep flow condition as sub-critical (i.e. Froude numbers less than unity). Flow conditions corresponded to values of the Reynolds number are $Re_h = U_{avg}d/\nu \approx 47{,}500$ & 31,000 and corresponded to Froude number are $F_r = U_{avg}/(gd)^{0.5} \approx 0.40$ & 0.24. Here, U_{avg} is the average velocity, d is the depth of flow, g is the acceleration due to gravity and ν is the kinematic viscosity of the fluid. Measured variation of water surface elevation was less than 1 mm over a streamwise distance of 600 mm implying a negligible pressure gradient. The summary of the test conditions was presented in Table I.

A commercial two-component fibre-optic LDA system (Dantec Inc.) powered by a 300-mW Argon-Ion laser was used for the velocity measurements. This system has been used in several previous studies and details are avoided for brevity [8], [22], [23]. The optical elements include a Bragg cell, a 500-mm focusing lens and the beam spacing was 38 mm. 10,000 validated samples were acquired at each measurement location. The data rate varied from 4 Hz to 65 Hz. Prior to the measurement of each set of data, the side wall of the flume was cleaned to minimize extraneous light scattered from particles distributed throughout the illuminating beams. Prior to the start of the measurements, the water was filtered for several days and then seeded with hollow spheres (Mean particle size = 12 microns and Density = 1.13 g/cc). The configuration of the present two-component LDA system

would not permit measurements very close to the wall, while one-component (streamwise velocity) measurements were made over the entire depth. The LDA probe was tilted 2° towards the bottom wall to capture near wall data for two-component velocity measurements. References [5], [15], have successfully adopted this procedure by tilting the probe by 3° and 2°, respectively, to allow data acquisition closer to the wall.

TABLE I
SUMMARY OF THE TEST CONDITIONS

Test	Bed Condition	U_{avg} (m/s)	d (mm)	R_{eh}	F_r
1	Smooth bed	0.375	~ 100	~ 47500	~ 0.40
2		0.24	~ 100	~ 31000	~ 0.24
3	Distributed roughness	0.357	~ 100	~ 47500	~ 0.40
4		0.24	~ 100	~ 31000	~ 0.24
5	Continuous roughness	0.358	~ 100	~ 47500	~ 0.40
6		0.23	~ 100	~ 31000	~ 0.24
7	Natural sand bed	0.40	~ 100	~ 47500	~ 0.40
8		0.25	~ 100	~ 31000	~ 0.24

III. RESULTS

Fig. 4 shows the Reynolds shear stress distribution on smooth and rough beds in outer variables for the lower Reynolds numbers. One can note from Fig. 4 that the Reynolds shear stress attains a maximum value at a location near the bed (y/d < 0.2). As expected, the flow over the rough beds generates higher near wall Reynolds shear stress than the smooth bed. The fixed continuous roughness condition shows the highest peak followed by distributed roughness and sand bed condition. However, in the outer region (y > 0.2d) the distributed roughness provides for the highest Reynolds shear stress followed by nearly same production by both continuous roughness and sand bed. Near the free surface, the Reynolds shear stress reduces and becomes negative for all bed conditions above the location where δU/δy is negative. Results indicate that the reduction of Reynolds shear stress from its maximum value is more or less linear for all surface conditions. One can clearly note from Fig. 4 that effect of bed condition on Reynolds stress is distinctly visible from near bed to the depth of flow as high as y ≈ 0.6d. However, [5], [24], [25] found the influence of bed condition on Reynolds shear stress penetrates up to y ≈ 0.2d ~ 0.3d. Reference [2] did not find any significant difference in their calculation of Reynolds shear stress for flow over smooth and rough bed (2 mm sand and 9 mm pebbles) and the outcome can be a result of very small number of sample size (~ 1000). The variation of Reynolds shear stress for the higher Reynolds number [20] shows a trend similar to that at the lower Reynolds. However, in this case the natural sand bed roughness shows the highest peak followed by distributed roughness bed and continuous roughness. Throughout the depth, distributed roughness bed also shows much more production of Reynolds shear stress than other rough beds. Enhanced Reynolds shear stress near rough beds resulted due to arrays of discrete roughness elements and flow over these scattered elements generates a series of wakes which contributes to this generation of significantly higher Reynolds shear stress.

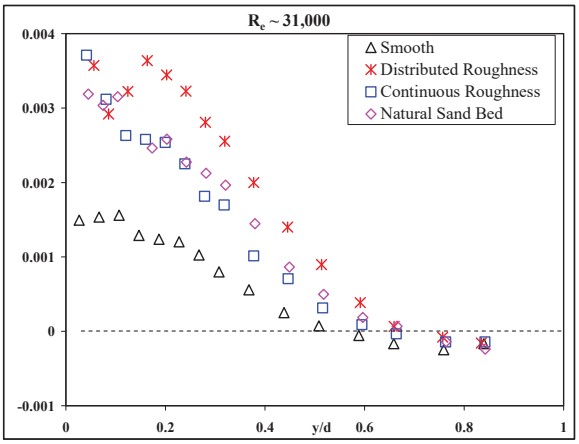

Fig. 4 Reynolds shear stress distribution for flow over different bed conditions

The distribution of different normalized velocity triple products $\overline{u^3}$, $\overline{u^2v}$, $\overline{v^3}$ and $\overline{v^2u}$, which provide valuable information about turbulence flow structures, are shown in Figs. 5 (a), (b), (c), and (d) respectively for the lower Reynolds numbers. Directly measured quantities like depth of flow and maximum velocity are used as the length and velocity scales, respectively, to reduce any additional uncertainties related to scaling parameters with computed quantities. One can define $\overline{u^3}$ and $\overline{v^2u}$ as streamwise flux and $\overline{u^2v}$ and $\overline{v^3}$ as wall normal transport/diffusion of the turbulent kinetic energy u^2 and v^2 respectively. $\overline{v^2u}$ is also defined as wall normal transport of the Reynolds shear stress. Velocity triple products provide information about ejection-sweep cycle, which is the main coherent motion responsible for most of the turbulent transport. Higher values of $\overline{u^3}$ relate to intense ejection/sweep events. One can also get an insight about change/modification of turbulent transport mechanism due to the change of bed condition by studying the variation of different velocity triple product.

One can note from Figs. 5 (a) and (b) that, for flow over a smooth bed, $\overline{u^3}$ is –ve and $\overline{u^2v}$ is +ve at the location very close to the bed. This indicates a slower moving fluid parcel with an upward transport of u momentum representing an ejection type motion. One can also note from Figs. 5 (a) and (b) that $\overline{u^3}$ and $\overline{u^2v}$ changes sign and become +ve and –ve respectively near the rough bed. Together with +ve and much higher value of $\overline{u^3}$ and -ve value of $\overline{u^2v}$ indicates a strong sweeping action motion in the streamwise direction that is partly directed towards the bed. As one progress from the bed towards the free surface, both parameters changes sign. Similar observation was made by [26] and relate this change with changes of ejection-sweep cycle and modification of the longitudinal vortices with accompanying low-speed streaks produced by the rough bed. As one move further from bed (y

> 0.08 d) the value of $\overline{u^3}$ become more negative causing the substantial reduction of sweep event and stay negative throughout the depth. One can also note the significant difference of $\overline{u^3}$ between smooth and rough bed throughout the flow depth. This is in direct contrast with [26], [27], who didn't observe much variation at distance y/d > 0.2. However, [28] found large differences of the variation of $\overline{u^3}$ for flows over transverse rod roughness up to the edge of boundary layer. Reference [2] related this difference to the lack of long streamwise vortices near the rough wall. Reference [2] also noted that the mechanics of the entrainment of low momentum fluid at the wall differed for rough bed conditions in comparison of the same for smooth wall. The trend of the variation of $\overline{v^3}$ (Fig. 5 (c)) is very similar to the variation of $\overline{u^2v}$ (Fig. 5 (b)) with the exception that $\overline{v^3}$ is positive throughout the depth and the magnitude is much smaller (~60%) than $\overline{u^2v}$. Comparing $\overline{v^2u}$ (Fig. 5 (d)) with $\overline{u^3}$ (Fig. 5 (a)), one can note qualitatively similar trend with magnitude of $\overline{v^2u}$ very much lower (20%~25%) than $\overline{u^3}$. References [5], [7] in their OCF experiments and [26], [27] in their TBL experiments had also noted similar reduction of value. The differences between $\overline{v^3}$ and $\overline{u^2v}$ and $\overline{v^2u}$ and $\overline{u^3}$ are mainly due to the less turbulent intensity in wall normal direction to that of streamwise direction. Although there are similarities about ratios of magnitude of different triple products between OCF and TBL but there are differences about the extent of depth affected by roughness, mainly in the outer layer due to free surface effect. One can note from Fig. 5 that the value of normalized different velocity triple products attains its local maximum/ minimum at the same location (≈ 0.25d to ≈ 0.30d). One can also note a 200% to 300% decrease/increase in magnitude of different velocity triple products between smooth and rough beds. Reference [7] also noticed significant decrease/increase (~ 300%) between smooth bed and flow over both smooth and rough dunes. This indicates that roughness has significant effect on the transportation of turbulent kinetic energy and Reynolds shear stress. As one move from local maximum/minimum level towards the free surface, values for different velocity triple products approaches to zero for all surfaces.

One can conclude from above discussion that the production of flux of turbulenct kinetic energy in streamwise direction is in excess of turbulent diffusion in normal to the bed, whereas, production of flux of turbulent kinetic energy normal to the bed is well absorbed by the turbulent diffusion in the streamwise direction. Moreover, the near-zero value of triple correlations near free surface is an indication of insignificant turbulent activity near free surface. One can also note that the location of local maximum/minimum in the profiles is independent of the type of roughness. Distributed roughness profile shows the greatest variation followed by similar variation for continuous roughness and sand bed. Near-bed (y < 0.1 d) turbulent activity also shows dependency on bed surface conditions, such that, ejection type activity was observed for flow over smooth bed, whereas sweeping type of activity was observed for flow over rough bed. If one were to extrapolate the above mentioned flow process to real field scenario, such strong sweeping or ejection motions of fluid parcels could influence resuspension and sediment transport. With exception of sweeping event observed at near-bed location of rough beds, ejection event was more prominent over the depth of flow. The strength of ejection event again depends on the bed surface condition, with distributed roughness shows more ejection events than other roughness conditions. The variation of velocity triple products for higher Reynolds number [20] is very much similar to that for lower Reynolds number (Fig. 5) and avoided here for brevity. However, towards the free surface, values for different velocity triple products approaches to zero for all surfaces except for $\overline{u^3}$ of distributed roughness. Distributed roughness shows significant turbulent activity even near free surface (y > 0.85d).

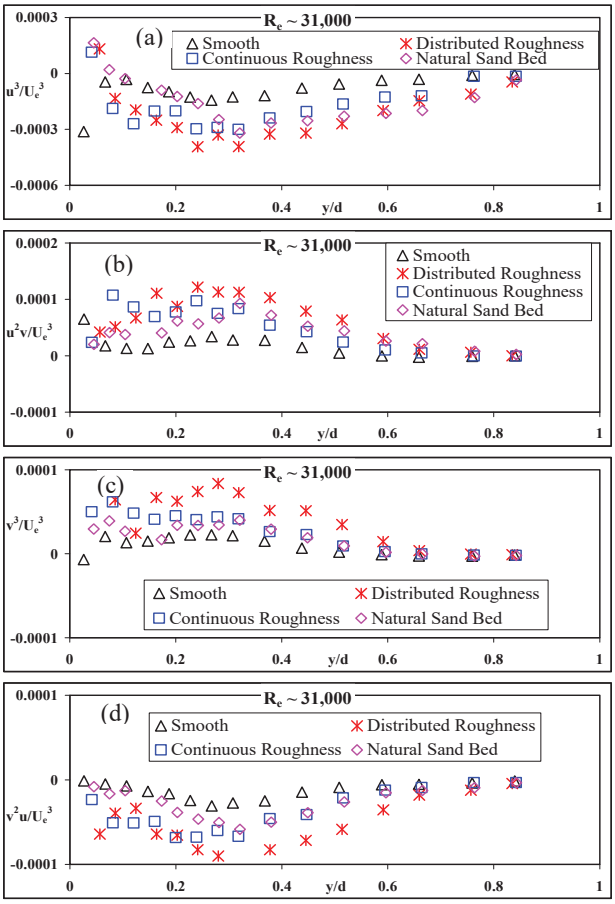

Fig. 5 Distribution of different velocity triple products for flow over different bed conditions

IV. Conclusion

An experimental study with four different types of bed conditions was carried out to understand the effect of

roughness in open channel flow at two different Reynolds numbers. The bed conditions include a smooth surface and three different roughness conditions which were generated using sand grains with a median diameter of 2.46 mm. The three rough conditions include a surface with distributed roughness, a surface with continuously distributed roughness and a sand bed with a permeable interface. A commercial two-component fibre-optic LDA system was used to conduct the velocity measurements. The variables of interest include the mean velocity, turbulence intensity, correlation between the streamwise and the wall normal turbulence, Reynolds shear stress and velocity triple products. The main findings are summarized as follows:

1. The flow over the rough beds generates higher near wall Reynolds shear stress than the smooth bed. The effect of bed condition on Reynolds shear stress is distinctly visible from near-bed to the depth of flow as high as $y \approx 0.7d$.
2. The result shows a 200% to 300% decrease/increase in magnitude of different velocity triple products between smooth and rough beds. This indicates that roughness has a significant effect on the transportation of turbulent kinetic energy and Reynolds shear stress.
3. Near-bed turbulent activity also shows dependency on bed surface conditions, such that, ejection type activity dominates for flow over smooth bed, whereas sweeping dominates for flow over the rough bed. If one were to extrapolate the above mentioned flow process to real field scenario, such strong sweeping or ejection motions of fluid parcels could influence resuspension and sediment transport.
4. With exception of sweeping events observed at near-bed location for rough beds, ejection events were more prominent over the depth of flow.
5. The strength of ejection event again depends on the bed surface condition, with distributed roughness showing more ejection events than other roughness conditions.
6. Existence of intermittent sweep and ejection events is universal but the extent of affected flow depth by either sweep or ejection is dependent on the bed and flow conditions.

REFERENCES

[1] Rashidi, M., Hetsroni, G., and Banerjee, S. (1990). "Particle-turbulence interaction in a boundary layer." *International Journal of Multiphase Flow,* 16(6), 935-949.

[2] Grass, A. J. (1971) "Structural features of turbulent flow over smooth and rough boundaries." *Journal of Fluid Mechanics,* 50(2), 233-255.

[3] Nakagawa, H. and Nezu, I. (1977). "Prediction of the contributions to the Reynolds stress from bursting events in open-channel flows." *Journal of Fluid Mechanics,* 80(1), 99-128.

[4] Nezu, I. and Nakagawa, H. (1993). *Turbulence in open-channel flows*. IAHR Monograph, A. A. Balkema, The Netherlands.

[5] Tachie, M. F. (2001). "Open-channel turbulent boundary layers and wall jets on rough surfaces." PhD thesis, University of Saskatchewan, Saskatchewan, Canada.

[6] Nezu, I. (2005). "Open-channel flow turbulence and its research prospect in the 21st century." *Journal of Hydraulic Engineering,* 131(4), 229-246.

[7] Balachandar, R., and Bhuiyan, F. (2007). "Higher-order moments of velocity fluctuations in an open channel flow with large bottom roughness." *Journal of Hydraulic Engineering,* 133(1), 77-87.

[8] Afzal, B., Faruque, M. A. A., and Balachandar, R. (2009). "Effect of Reynolds number, near-wall perturbation and turbulence on smooth open channel flows." *Journal of Hydraulic Research*, 47(1), 66-81.

[9] Patel V. C. (1998). "Perspective: Flow at high Reynolds number and over rough surfaces – Achilles heel of CFD." *Journal of Fluids Engineering,* 120(3), 434-444.

[10] Roussinova, V., Biswas, N., and Balachandar, R. (2008). "Revisiting turbulence in smooth uniform open channel flow." *Journal of Hydraulic Research*, 46(Suppl. 1), 36-48.

[11] Kirkgöz, M. S., and Ardiçhoğlu, M. (1997). "Velocity profiles of developing and developed open channel flow." *Journal of Hydraulic Engineering,* 123(2), 1099-1105.

[12] Tachie, M. F., Bergstrom, D. J., and Balachandar, R. (2003). "Roughness effects in low-Re_τ open-channel turbulent boundary layers." *Experiments in Fluids,* 35, 338-346.

[13] Balachandar, R., and Patel, V. C. (2002). "Rough wall boundary layer on plates in open channels." *Journal of Hydraulic Engineering,* 128(10), 947-951.

[14] Tachie, M. F., Bergstrom, D. J., and Balachandar, R. (2000). "Rough wall turbulent boundary layers in shallow open channel flow." *Journal of Fluids Engineering,* 122, 533-541.

[15] Kaftori, D., Hetsroni, G., and Banerjee, S. (1995). "Particle behavior in the turbulent boundary layer. I. Motion, deposition, and entrainment." *Physics of Fluids,* 7(5), 1095-1106.

[16] Dancey, C. L., Balakrishnan, M., Diplas, P., and Papanicolaou, A. N. (2000). "The spatial inhomogeneity of turbulence above a fully rough, packed bed in open channel flow." *Experiments in Fluids,* 29(4), 402-410.

[17] Tachie, M. F., Bergstrom, D. J., and Balachandar, R. (2004). "Roughness effects on the mixing properties in open channel turbulent boundary layers." *Journal of Fluids Engineering,* 126, 1025-1032.

[18] Bigillon, F., Niño, Y., and Garcia, M. H. (2006). "Measurements of turbulence characteristics in an open-channel flow over a transitionally-rough bed using particle image velocimetry." *Experiments in Fluids,* 41(6), 857-867.

[19] Dancey, C. L., Balakrishnan, M., Diplas, P., and Papanicolaou, A. N. (2000). "The spatial inhomogeneity of turbulence above a fully rough, packed bed in open channel flow." *Experiments in Fluids,* 29(4), 402-410.

[20] Faruque, M. A. A. (2009). "Smooth and rough wall open channel flow including effects of seepage and ice cover." PhD thesis, University of Windsor, Windsor, ON, Canada.

[21] Schlichting, H. (1979). *Boundary-Layer theory*. McGraw-Hill Classic Textbook Reissue Series, McGraw-Hill, Inc., United States of America.

[22] Faruque, M. A. A., Sarathi, P., and Balachandar, R. (2006). "Clear water local scour by submerged three-dimensional wall jets: Effect of tailwater depth." *Journal of Hydraulic Engineering,* 132(6), 575-580.

[23] Bey, A., Faruque, M. A. A., and Balachandar, R. (2007). "Two dimensional scour hole problem: Role of fluid structures." *Journal of Hydraulic Engineering,* 133(4), 414-430.

[24] Krogstad, P.-A., Andersson, H. I., Bakken, O. M., and Ashrafian, A. (2005). "An experimental and numerical study of channel flow with rough walls." *Journal of Fluid Mechanics,* 530, 327-352.

[25] Agelinchaab, M., and Tachie, M. F. (2006). "Open channel turbulent flow over hemispherical ribs." *International Journal of Heat and Fluid Flow,* 27(6), 1010-1027.

[26] Schultz, M. P. and Flack, K. A. (2007). "The rough-wall turbulent boundary layer from the hydraulically smooth to the fully rough regime." *Journal of Fluid Mechanics,* 580, 381-405.

[27] Flack, K. A., Schultz, M. P. and Shapiro, T. A. (2005). "Experimental support for Townsend's Reynolds number similarity hypothesis on rough walls." *Physics of Fluids,* 17(3), 35102-1-9.

[28] Antonia, R. A., and Krogstad, P-A. (2001). "Turbulence structure in boundary layers over different types of surface roughness." *Fluid Dynamics Research,* 28(2), 139-157.